Nanoscale

Accepted Manuscript

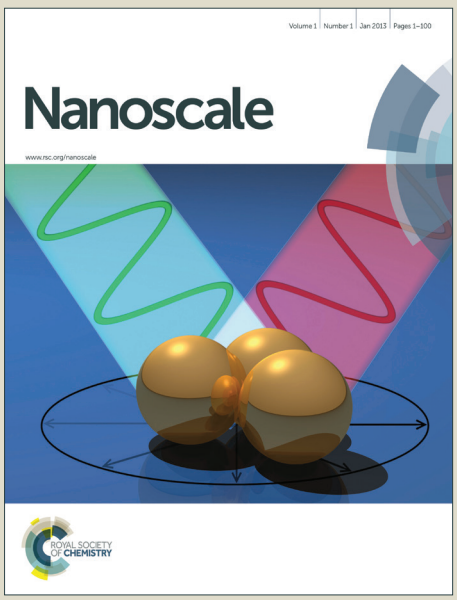

ROYAL SOCIETY OF CHEMISTRY

www.rsc.org/nanoscale

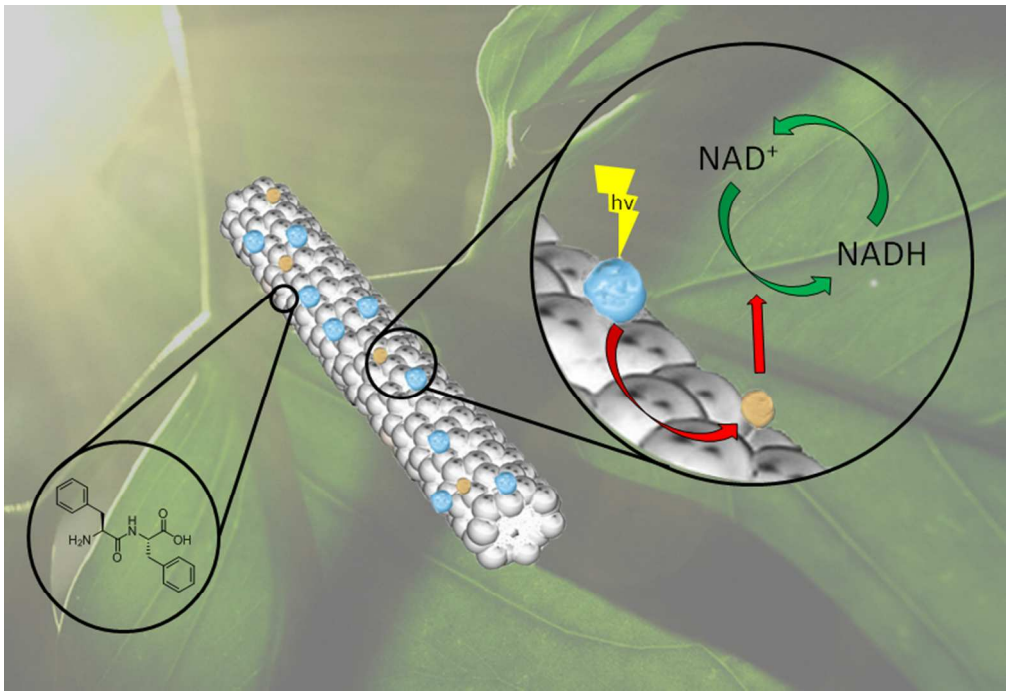

graphic abstract
229x157mm (96 x 96 DPI)

Nanoscale

RSCPublishing

COMMUNICATION

Integrated artificial photosynthesis system based on peptide nanotubes†

Cite this: DOI: 10.1039/x0xx00000x

Bin Xue, [a] Ying Li, [a, b] Fan Yang, [a] Chunfeng Zhang, [a] Meng Qin*, [a] Yi Cao*, [a] and Wei Wang* [a]

Received 00th January 2012,
Accepted 00th January 2012

DOI: 10.1039/x0xx00000x

www.rsc.org/

A peptide nanotube platform that integrates both light-harvesting and catalysis units was successfully engineered for artificial photosynthesis. Peptide nanotubes not only serve as a hub for physically combining both units, but also work as mediators that transfer the energy from photo-excited chromophores to catalytic centers. The direct conversion of NAD^+ to NADH upon light illumination was demostrated. This represents a promising step towards efficient and fully integrated artificial photosynthesis systems.

Solar energy is the most abundant, sustainable, and environmentally friendly source of energy on the earth.[1, 2] Many plants and bacteria are able to efficiently convert photo energy from sunlight to chemical energy using their sophisticated photosynthesis system. A hallmark of such photosynthesis system is the precise arrangement of the light harvesting antenna chromophores and the catalytic centers.[3-5] This allows the efficient electronic energy-transfer from the photo-excited chromophores to the catalytic metal clusters for chemical reactions.[6, 7] Inspired by the natural photosynthesis, tremendous efforts have been made for the design of artificial photosynthesis system.[8-14] However, most studies so far are focused on mimicking the natural light harvesting process.[15-29] The development of fully integrated photosynthesis system has only been reported in very few cases,[30-37] because uniting light-harvesting and chemical or biological catalysis centers in a single system is technically challenging. The integrated system requires precisely placing different parts without crosstalk between individual assembly processes. Moreover, it requires a predefined energy circuit that allows the energy harvested by photo-excited chromophores to quickly and efficiently transfer to the catalytic units. In a recent elegant work by Park group,[33] they introduced a peptide-nanotube-based platform for artificial photosynthesis. However, due to the unmatched energy levels between the photo-harvesting unit and the catalysis unit, an electron mediator in the solution is still required for the energy flow. It is desirable to further harnessing such system to achieve more efficient photo-catalysis. To this end, here we reported a successful self-assembled peptide-nanotube-based system which integrates ruthenium-based light harvesting units with the platinum catalytic centers without the need of any electron mediators. Moreover, this system exhibits high turnover frequency, tunable energy gap, and low toxicity, representing a promising artificial photosynthesis system with great potential applications.

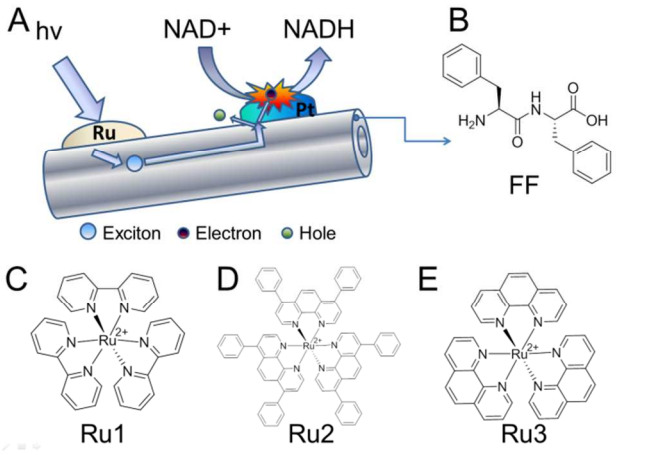

Fig. 1. Schematic of the peptide nanotube based artificial photosynthesis system. (A) Proposed energy flow between the light harvesting unit (Ruthenium complex) and the catalysis unit (Platinum nanoparticle). (B) The structure of diphenylalanine (FF) that constitutes of the peptide nanotubes. (C), (D), and (E) The molecular structures of three ruthenium complexes used in this study.

The design of the artificial photosynthesis system is pictorially illustrated in Fig. 1A. We chose diphenylalanine (FF) peptide nanotubes as the platform for the integration because they are extremely stable in different solvent conditions, highly conductive, and easy to fabricate.[38-43] In addition, ruthenium-based light harvesting molecules have been widely developed and are among one of the most promising artificial light harvesting chromophores, because of their exceptional photo-stability, broad absorption in the visible

region, and relatively long-lived excited states.[44-48] In this work, we studied three different types of ruthenium complexes as potential light-harvesting units (Fig. 1C, D and E) to screen for the most suitable candidate. Due to strong hydrophobic interactions between the hydrophobic ligands with FF, these ruthenium complexes can be adequately attached to the surface of FF nanotubes. The catalytic centers, platinum clusters, can be easily implemented onto the surface of FF nanotubes by in situ metallization. The proposed energy flow is shown in Fig. 1A. First, Ruthenium ions absorb sunlight and generate excitons, which subsequently migrate to FF nanotubes through ligands. Because FF nanotubes are suitable for exciton transport, as evidenced from DFT calculations, [49] the excitons may reach platinum nanoparticles in distance. Subsequently, the platinum nanoparticles separate the excitons into electrons and holes and catalyze the reduction of nicotinamide adenine dinucleotide (NAD^+) to NADH, which can be subsequently used in the Calvin cycle.

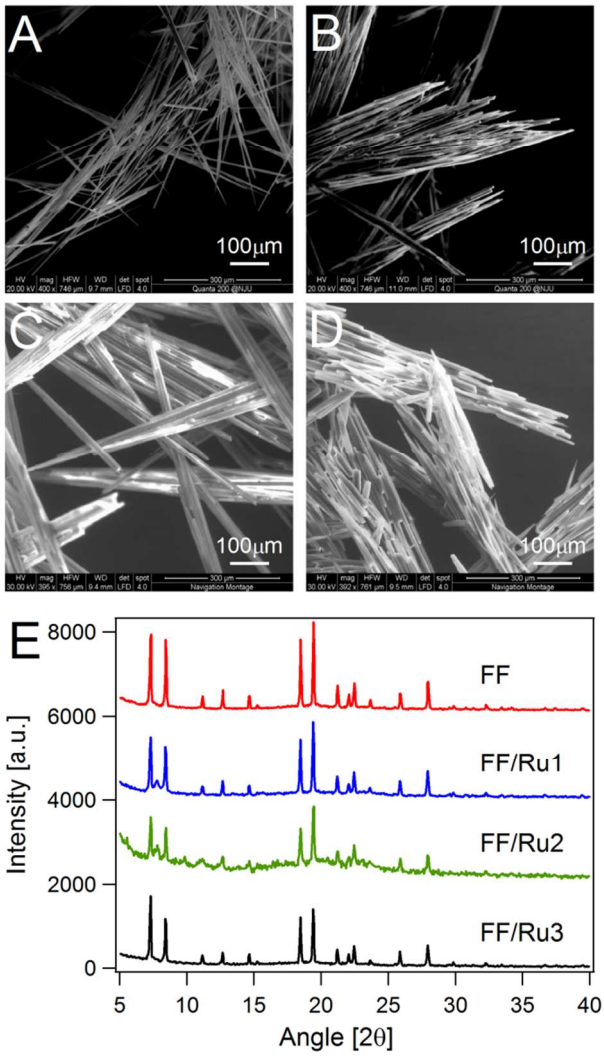

Fig. 2. Structures of FF/Ru nanotubes. (A)-(D) SEM images of FF, FF/Ru1, FF/Ru2, and FF/Ru3. FF/Ru nanotubes retain similar structures as FF nanotubes. (E) XRD of FF, FF/Ru1, FF/Ru2, and FF/Ru3. Incorporation of Ruthenium complexes to FF nanotubes does not change the molecular arrangement of FF peptides in the nanotubes.

We first prepared the ruthenium complex decorated FF nanotubes in the phosphate buffer (PB, 100 mM, pH 6.0). The FF nanotubes was fabricated by first dissolving FF peptides in 1,1,1,3,3,3-hexafluoro-2-propanol (HFIP) at a concentration of (100 mg mL^{-1}) and then diluting the solution into a phosphate buffer (PB) at a final concentration of 2mg mL^{-1}. White fibrous precipitates formed immediately upon the addition of the FF solution to PB buffer (Fig. S1). The structure of the FF tubes was studied using scanning electron microscope (SEM). FF assembled into straight nanotubes of more than 500 μm long with diameters of 500-2000 nm as shown in Fig. 2A. The FF nanotubes were conductive and could be imaged without gold sputter coating. Adding FF nanotubes to solutions containing 1 mg mL^{-1} ruthenium complexes Ru1, Ru2, and Ru3 (Fig. 1C, D, and E) caused the deposition of ruthenium complexes on the surfaces of FF nanotubes. The color of the ruthenium complex solutions became lighter and the FF nanotubes were in yellow or brown color (Fig. S1). The SEM images of these FF/Ru tubes are shown in Fig. 2B, C, and D. Clearly, the morphologies of these nanotubes were almost unchanged. We proposed that ruthenium complexes may reside on the surface of FF nanotubes. Due to the deposition of ruthenium complexes and the increase of surface hydrophobicity, the tubes tended to form large bundles. The presence of ruthenium ligands on the FF nanotube surfaces was also evidenced from the energy dispersive X-ray analysis (EDX, Fig. S2). More importantly, deposition of ruthenium complexes on the surface of FF nanotubes did not change the molecular arrangement of FF peptides in the nanotubes. As shown in Fig. 2E, the x-ray diffraction (XRD) pattern of these FF/Ru tubes resembled the unmodified FF nanotubes.[42, 50] Notably, due to different hydrophobicity of the three ruthenium complexes, they showed distinct morphologies on FF nanotubes, as revealed by transmission electron microscope (TEM, Fig. S3). Ru1 and Ru3 distributed on the surface of FF nanotubes homogeneously and were not visible, while Ru2 formed clusters due to its higher hydrophobicity. Moreover, the addition of Ru2 led to thinner FF nanotubes.

To evaluate the light harvesting capabilities of the FF/Ru nanotubes, we measured their photoelectric properties. We first probed the effects of FF nanotubes to the fluorescence lifetimes of ruthenium compounds. The addition of FF nanotubes greatly decreased the lifetime of all ruthenium complexes. The lifetime for Ru1 decreases from 59 ns to 9.6 ns; the lifetime for Ru2 decreases from 3.5 ns to 1.1 ns; and the lifetime for Ru3 decreases from 12 ns to 8.8 ns. This indicates that upon deposition on the FF nanotubes, the energy harvested by the ruthenium complexes upon light illumination can be efficiently transferred either directly to the FF nanotubes or through other non-radiative relaxation channels at nanosecond time scale. We also tested whether the formation of FF/Ru nanotubes changes the optical properties of the ruthenium complexes. The UV-Vis spectra of ruthenium complexes did not change upon coupling with FF nanotubes (Fig. S4), suggesting the light absorption properties of ruthenium complexes were not affected. The fluorescence emission spectra were almost unaltered for Ru1 and Ru3 when interacting with FF nanotubes (Fig. S5), indicating that the quantum yields of Ru1 and Ru3 remained the same. However, the fluorescence of Ru2 increases by 3 times in the presence of FF. This is probably due to strong hydrophobic interactions between the ligand of Ru2 and FF nanotubes, which leads to an increase in its quantum yield. The emission maxima for Ru1 and Ru3 also remained the same, suggesting that the energy gap corresponding to the metal-to-ligand charge

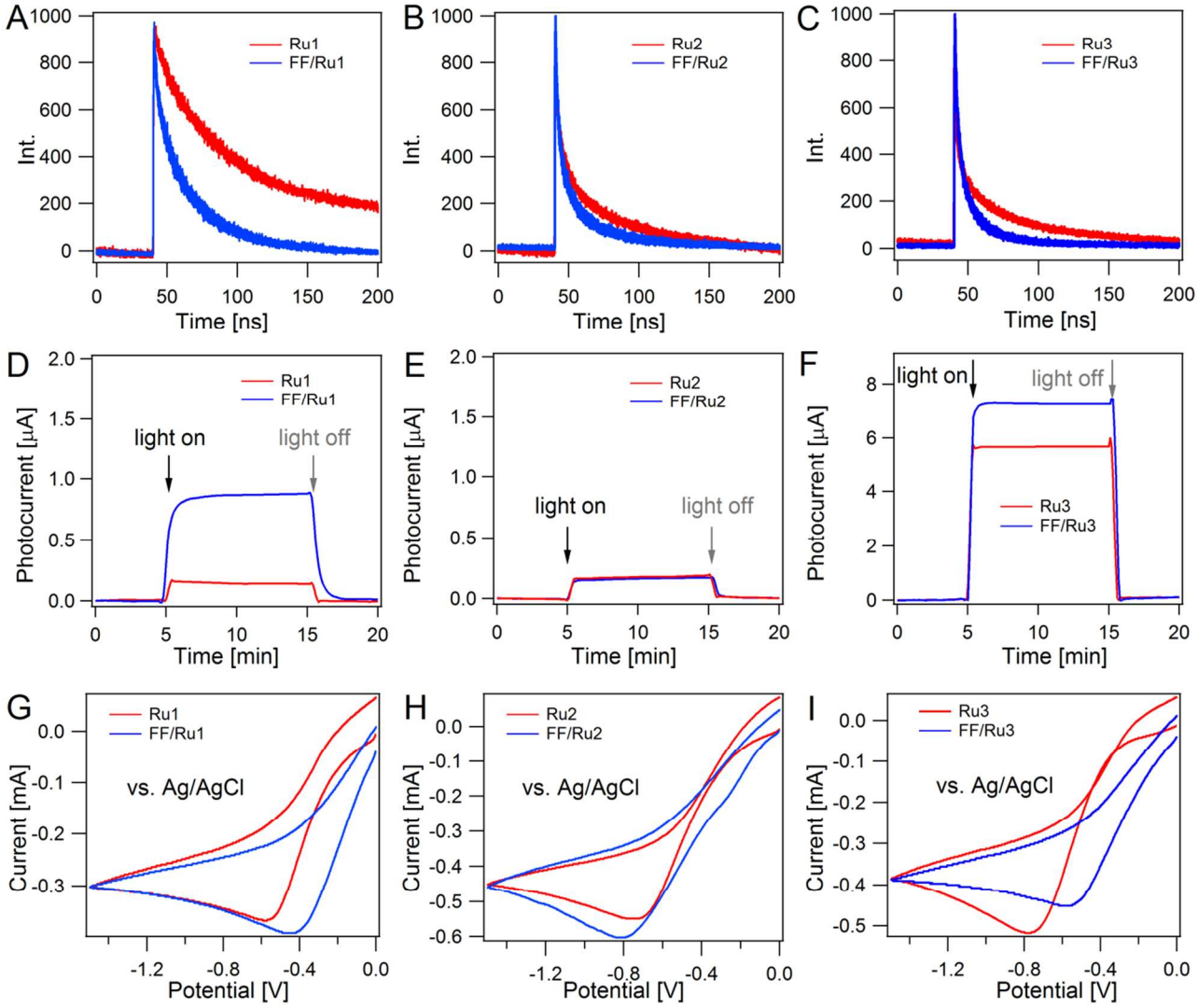

Fig. 3 Spectroscopic and photoelectric properties of FF/Ru nanotubes. (A)-(C) Time-resolved phosphorescence decays of Ru1, FF/Ru1, Ru2, FF/Ru2, Ru3, and FF/Ru3 (exited at 405 nm). The total counts of each trace were kept the same and the intensity did not correspond to the fluorescence property of the samples. (D)-(F) Photocurrent response of ruthenium complexes in the absence and presence of FF nanotubes on an ITO electrode (1 cm^2). Black arrows indicate light-on and gray arrows indicate the light-off, respectively. (G)-(I) Cyclic voltammogram of Ruthenium complex and FF/Ru nanotubes with a scan rate of 100 mV s^{-1}.

transfer (MLCT) were not altered upon their interaction with FF nanotubes.[51] However for Ru2, the energy gap became broader as the emission peak was blue-shifted in the presence of FF nanotubes. We then studied the photocurrent response of the FF/Ru nanotubes on an indium tin oxide (ITO) glass anode in the PB buffer containing 15% (w/v) triethanolamine (TEOA) as an electron donor upon white light illumination. As shown in Fig. 3D, E and F, the intrinsic photocurrent is the highest for Ru3 and the lowest for Ru1. However, upon the adsorption on FF nanotubes, the photocurrent of Ru1 is enhanced by ~ 3 folds. The increase of photocurrents suggested that direct ligand-nanotube interactions might facilitate the delocalization of excitons and suppress electron-hole recombination. For Ru2, the photocurrent is almost unchanged; and for Ru3, the photocurrent only increased by ~30%. Although the change of photocurrents of the ruthenium ligands upon interactions with FF nanotubes cannot be predicted *a priori*, these characterizations served as the basis for the understanding of energy flow in the artificial photosynthesis system. To get more insights into the energetic flow between ruthenium complexes and FF nanotubes, we also measured the redox of Ru1, Ru2, and Ru3 using cyclic voltammetry (Fig. 3G, H and I). The reduction peaks for Ru1, Ru2 and Ru3 alone locate at -0.57 V, -0.55 V and -0.58 V, respectively. However, the reduction peaks for the ruthenium complexes are significantly altered upon interactions with FF nanotubes. With FF nanotubes, the reduction peaks for Ru1 and Ru3 positively shifted to -0.42 V and -0.45 V, respectively. This suggests that the electron flow from Ru1 and Ru2 to the catalytic centers is promoted upon interactions with FF nanotubes. However, for Ru3, coupling with FF nanotubes made its reduction peak more negative, which indicates that the energy gap became bigger.

We then integrated the catalytic centers, platinum nanoparticles (Pt-NPs) onto the light-harvesting FF-nanotubes by *in situ* self-metallization. FF/Ru nanotubes were redispersed in the PB buffer (100 mM, pH 6.0) containing K_2PtCl_4 (7 mM)

and ascorbic acid (7 mM). Then the reduction of platinum was triggered by the exposure to visible light for 30 min. The color of the nanotubes became slightly darker when Pt-NPs formed on their surface (Fig. S6). The morphologies of the FF/Ru nanotubes were not affected by the deposition of Pt-NPs, as shown in Fig. 4A, B and C. However, the deposition of Pt-NPs led to partial aggregation of the nanotubes to spindle-like bundles. The presence of Pt-NPs on these nanotubes was also confirmed by EDX. (Fig. S2) The formation of Pt-NPs on the surface of FF nanotubes can be directly viewed by TEM. (Fig. S3) Deposition of Pt-NPs did not change the molecular arrangement of FF nanotubes, as revealed by XRD analysis of FF/Ru/Pt nanotubes. (Fig. S7) Incorporation of Pt-NPs could lead to significant increase of the redox current and shifts of the reduction potentials of FF/Ru nanotubes (Fig. S8). For FF/Ru1/Pt and FF/Ru2/Pt, the signals are dominated by that from Pt-NPs. It seems that the redox potential for FF/Ru3/Pt is distinct from FF/Ru1/Pt and FF/Ru2/Pt, probably because less Pt-NP was formed.

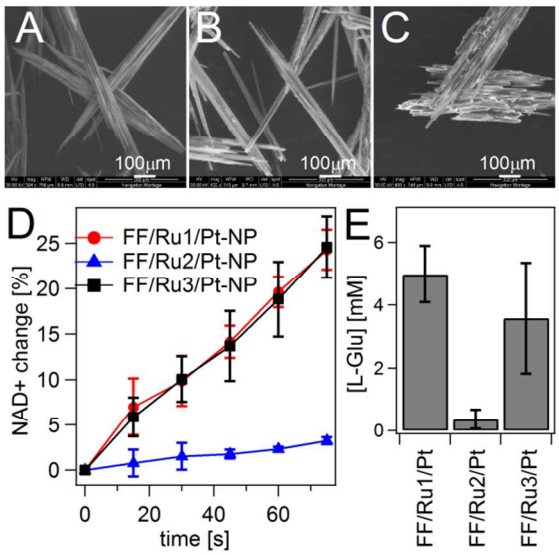

Fig. 4. Photo-catalysis of FF/Ru/Pt nanotubes. (A)-(C) SEM images of FF/Ru1/Pt, FF/Ru2/Pt, and FF/Ru3/Pt nanotubes. (D) Photo-reduction of NAD^+ to NADH catalyzed by FF/Ru/Pt nanotubes. Conditions: 1 mM NAD^+, 100 mM ammonium sulphate, and 15 w/v% TEOA in a phosphate buffer (100 mM, pH 6.0). (E) Conversion of α-ketoglutarate to L-glutamate by the glutamate dehydrogenase (GDH) coupled to the FF/Ru/Pt photosynthesis systems in 1 h. Conditions: 1 mM NAD^+, 5 mM α-ketoglutarate, 100 mM ammonium sulphate, 50 U GDH, and 15 w/v% TEOA in a phosphate buffer (100 mM, pH 6.0).

Having successfully synthesized these FF/Ru/Pt nanotubes, we were ready to test the conversion of photo energy to chemical energy using this artificial photosynthesis system. To mimic the light reaction of photosynthesis, we studied the FF/Ru/Pt nanotubes catalyzed light driven conversion of NAD^+ to NADH in the presence of the electron donor TEOA. We used the UV-Vis spectra to monitor this reaction in real time. (Fig. S9) The reaction occurred only in the presence of both ruthenium complexes and Pt-NPs. Moreover, without FF nanotubes, no reaction took place because of the lack of the photo electron flow pathway. (Fig. S10) The three types of FF/Ru/Pt nanotubes showed distinct catalysis behaviors. Upon exposure to visible light (~13.5 mW cm^{-2}) for 75 min, ~24.6% and ~24.2% NAD^+ were converted to NADH for Ru1 and Ru3 decorated FF/Ru/Pt nanotubes, respectively. (Fig. 4D) However, Ru2 decorated FF/Ru/Pt nanotubes showed only 3.2% conversion. (Fig. 4D) The distinct catalytic activity was not only due to the intrinsic light harvesting ability of these three compounds but also related to the energy transport from the ruthenium complex to the Pt nanoparticles. For example, Ru1 exhibits 9 times less photocurrent yet shows similar catalytic activity as compared to Ru3 due to its unique electron migration pathway. These results highlighted the importance in the design of the energy flow in the artificial photosynthesis system. The turnover frequencies of FF/Ru/Pt were estimated to be 3.71 h^{-1}, 0.48 h^{-1}, and 3.65 h^{-1}, respectively. The turnover frequencies for Ru1, Ru3 decorated nanotubes outperformed that of THPP based peptide nanotubes (1.78 h^{-1}), CdTe quantum dots (0.540 h^{-1}), CdSe quantum dots (0.158 h^{-1}), and p-doped TiO_2 (0.003 h^{-1}). [33] Therefore, the peptide nanotube-based artificial photosynthesis system reported herein could have promising potential applications. Comparing to carbon nanotube (CNT)-based photosynthesis systems the peptide-based system reported here may be also advantageous, because peptide nanotubes are more reactive than CNT, making the functionalization of the nanotubes much easier. Moreover, the photoelectric properties of the peptide nanotube-based system are tunable by changing the structure of the peptide molecules.

As a proof-of-principle demonstration, we coupled the photo catalysis by FF/Ru/Pt-NP to an enzymatic reaction by the glutamate dehydrogenase (GDH), which utilizes NADH for the conversion of α-ketoglutarate to L-glutamate (L-Glu). The production of L-Glu after 1 h of reaction using the three different artificial photosynthesis systems was summarized in Fig. 4E. The L-Glu generated using FF/Ru1/Pt was the highest, indicating that more catalytic active NADH was produced. Although FF/Ru3/Pt showed similar catalytic activity for the reduction of NAD^+, some side products, such as NADH isomers or dimers, instead of 1, 4 NADH might be also produced, which cannot be used for the conversion of α-ketoglutarate to L-Glu. Therefore, less L-Glu was produced in the FF/Ru3/Pt system. We proposed that this is probably because the lack of efficient electron mediators in this system. [52] Tuning the relative redox energetics between ruthenium complexes and peptide nanotubes is crucial for the applications of such artificial photosynthesis system. It is also worth mentioning that because the peptide nanotubes were suspended in the solution, recycling the catalysts for multiple runs of photoreaction is also difficult. We are currently exploring hydrogel based artificial photosynthesis system to improve the recyclability.

Conclusions

In summary, in this work, we successfully used peptide-based nanotubes as a novel platform for the engineering of artificial photosynthesis system. The light harvesting unit, ruthenium complex, and the catalytic unit, platinum nanoparticles, were successfully integrated into diphenylalanine nanotubes. The light harvesting capabilities of the ruthenium complex can be affected by the interactions between the ligands and the diphenylalanine nanotubes. By comparing the catalytic activity of different ruthenium complexes, we demonstrated that the overall catalytic activity is not only dependent on the light harvesting capability of these compounds but also related

to the energy flow along the entire artificial photosynthesis system. We were able to efficiently convert photo energy to chemical energy using this system without the aid of additional electron mediators. It is possible to finely tune the efficiency of the photo-catalysis by further engineering the ruthenium ligands for optimized energy flow. Given that many novel ruthenium ligands available in literature, we are confident that the catalytic efficiency of this system can be further improved. Moreover, with the improved peptide design, precisely placing the light harvesting units and the catalytic units onto peptide nanotubes with much ordered structures should be also achievable in the near future. Therefore, this work represents a novel and promising direction towards the engineering of efficient and fully integrated artificial photosynthesis systems. Real photosynthesis systems of plants and a few bacteria are much more complicated that artificial ones. There is still a long way ahead for the engineering of artificial photosynthesis systems of similar photochemical properties as the naturally occurring ones.

Acknowledgements

We thank Prof. Chunfeng Zhang for the fluorescence lifetime measurements. This work was supported by the 973 Program of China (no. 2012CB921801), the NSFC, under grant no. 11374148, 11304156, and 11334004, and the Priority Academic Program Development of Jiangsu Higher Education Institutions. Y.L. was supported by CPSF (2013M531312) granted of China.

Notes and references

[a] National Laboratory of Solid State Microstructure, Department of Physics, Nanjing University 22 Hankou Road, Nanjing, Jiangsu, China, 210093 Fax: (+86)83595535 E-mail: caoyi@nju.edu.cn, qinmeng@nju.edu.cn or wangwei@nju.edu.cn

[b] Jiangsu Key Laboratory of Atmospheric Environment Monitoring & Pollution Control, College of Environmental Science & Engineering Nanjing University of Information Science & Technology 219 Ningliu Road, Nanjing, Jiangsu, China 210044

† Electronic Supplementary Information (ESI) available: [Experimental procedures and supporting figures]. See DOI: 10.1039/c000000x/

1. A. W. Larkum, *Curr Opin Biotechnol*, 2010, **21**, 271-276.
2. R. E. Blankenship, D. M. Tiede, J. Barber, G. W. Brudvig, G. Fleming, M. Ghirardi, M. R. Gunner, W. Junge, D. M. Kramer, A. Melis, T. A. Moore, C. C. Moser, D. G. Nocera, A. J. Nozik, D. R. Ort, W. W. Parson, R. C. Prince and R. T. Sayre, *Science*, 2011, **332**, 805-809.
3. A. Amunts, O. Drory and N. Nelson, *Nature*, 2007, **447**, 58-63.
4. P. Jordan, P. Fromme, H. T. Witt, O. Klukas, W. Saenger and N. Krauss, *Nature*, 2001, **411**, 909-917.
5. A. Zouni, H. T. Witt, J. Kern, P. Fromme, N. Krauss, W. Saenger and P. Orth, *Nature*, 2001, **409**, 739-743.
6. I. McConnell, G. Li and G. W. Brudvig, *Chem Biol*, 2010, **17**, 434-447.
7. G. D. Scholes, G. R. Fleming, A. Olaya-Castro and R. van Grondelle, *Nat Chem*, 2011, **3**, 763-774.
8. M. S. Choi, T. Yamazaki, I. Yamazaki and T. Aida, *Angew Chem Int Ed Engl*, 2004, **43**, 150-158.
9. A. Ajayaghosh, V. K. Praveen and C. Vijayakumar, *Chem Soc Rev*, 2008, **37**, 109-122.
10. D. Gust, T. A. Moore and A. L. Moore, *Acc Chem Res*, 2009, **42**, 1890-1898.
11. M. R. Wasielewski, *Acc Chem Res*, 2009, **42**, 1910-1921.
12. K. Kalyanasundaram and M. Graetzel, *Curr Opin Biotechnol*, 2010, **21**, 298-310.
13. J. Barber, *Chem Soc Rev*, 2009, **38**, 185-196.
14. J. J. Concepcion, R. L. House, J. M. Papanikolas and T. J. Meyer, *Proc Natl Acad Sci U S A*, 2012, **109**, 15560-15564.
15. L. Chen, Y. Honsho, S. Seki and D. Jiang, *J Am Chem Soc*, 2010, **132**, 6742-6748.
16. H. Q. Peng, Y. Z. Chen, Y. Zhao, Q. Z. Yang, L. Z. Wu, C. H. Tung, L. P. Zhang and Q. X. Tong, *Angew Chem Int Ed Engl*, 2012, **51**, 2088-2092.
17. J. G. Woller, J. K. Hannestad and B. Albinsson, *J Am Chem Soc*, 2013, **135**, 2759-2768.
18. A. Ajayaghosh, V. K. Praveen, C. Vijayakumar and S. J. George, *Angew Chem Int Ed Engl*, 2007, **46**, 6260-6265.
19. C. V. Kumar and M. R. Duff, Jr., *J Am Chem Soc*, 2009, **131**, 16024-16026.
20. R. A. Miller, N. Stephanopoulos, J. M. McFarland, A. S. Rosko, P. L. Geissler and M. B. Francis, *J Am Chem Soc*, 2010, **132**, 6068-6074.
21. Y. S. Nam, T. Shin, H. Park, A. P. Magyar, K. Choi, G. Fantner, K. A. Nelson and A. M. Belcher, *J Am Chem Soc*, 2010, **132**, 1462-1463.
22. Y. Liang, P. Guo, S. V. Pingali, S. Pabit, P. Thiyagarajan, K. M. Berland and D. G. Lynn, *Chem Commun (Camb)*, 2008, 6522-6524.
23. H. Imahori, *J Phys Chem B*, 2004, **108**, 6130-6143.
24. K. J. Channon, G. L. Devlin and C. E. MacPhee, *J Am Chem Soc*, 2009, **131**, 12520-12521.
25. H. Takeda, Y. Goto, Y. Maegawa, T. Ohsuna, T. Tani, K. Matsumoto, T. Shimada and S. Inagaki, *Chem Commun (Camb)*, 2009, 6032-6034.
26. I. Nabiev, A. Rakovich, A. Sukhanova, E. Lukashev, V. Zagidullin, V. Pachenko, Y. P. Rakovich, J. F. Donegan, A. B. Rubin and A. O. Govorov, *Angew Chem Int Ed Engl*, 2010, **49**, 7217-7221.
27. S. Inagaki, O. Ohtani, Y. Goto, K. Okamoto, M. Ikai, K. Yamanaka, T. Tani and T. Okada, *Angew Chem Int Ed Engl*, 2009, **48**, 4042-4046.
28. K. V. Rao, K. K. Datta, M. Eswaramoorthy and S. J. George, *Angew Chem Int Ed Engl*, 2011, **50**, 1179-1184.
29. J. W. Springer, P. S. Parkes-Loach, K. R. Reddy, M. Krayer, J. Jiao, G. M. Lee, D. M. Niedzwiedzki, M. A. Harris, C. Kirmaier, D. F. Bocian, J. S. Lindsey, D. Holten and P. A. Loach, *J Am Chem Soc*, 2012, **134**, 4589-4599.
30. B. Rybtchinski, L. E. Sinks and M. R. Wasielewski, *J Am Chem Soc*, 2004, **126**, 12268-12269.

31. K. Maeda, M. Eguchi, S.-H. A. Lee, W. J. Youngblood, H. Hata and T. E. Mallouk, *The Journal of Physical Chemistry C*, 2009, **113**, 7962-7969.
32. Y. S. Nam, A. P. Magyar, D. Lee, J. W. Kim, D. S. Yun, H. Park, T. S. Pollom, Jr., D. A. Weitz and A. M. Belcher, *Nat Nanotechnol*, 2010, **5**, 340-344.
33. J. H. Kim, M. Lee, J. S. Lee and C. B. Park, *Angew Chem Int Ed Engl*, 2012, **51**, 517-520.
34. J. Ryu, S. H. Lee, D. H. Nam and C. B. Park, *Adv Mater*, 2011, **23**, 1883-1888.
35. M. Lee, J. H. Kim, S. H. Lee and C. B. Park, *ChemSusChem*, 2011, **4**, 581-586.
36. S. H. Lee, J. H. Kim and C. B. Park, *Chemistry*, 2013, **19**, 4392-4406.
37. R. K. Yadav, J. O. Baeg, G. H. Oh, N. J. Park, K. J. Kong, J. Kim, D. W. Hwang and S. K. Biswas, *J Am Chem Soc*, 2012, **134**, 11455-11461.
38. M. Reches and E. Gazit, *Science*, 2003, **300**, 625-627.
39. L. Adler-Abramovich, M. Reches, V. L. Sedman, S. Allen, S. J. Tendler and E. Gazit, *Langmuir*, 2006, **22**, 1313-1320.
40. N. Kol, L. Adler-Abramovich, D. Barlam, R. Z. Shneck, E. Gazit and I. Rousso, *Nano Lett*, 2005, **5**, 1343-1346.
41. N. Amdursky, M. Molotskii, D. Aronov, L. Adler-Abramovich, E. Gazit and G. Rosenman, *Nano Lett*, 2009, **9**, 3111-3115.
42. M. Wang, S. Xiong, X. Wu and P. K. Chu, *Small*, 2011, **7**, 2801-2807.
43. T. Andrade-Filho, F. F. Ferreira, W. A. Alves and A. R. Rocha, *Phys Chem Chem Phys*, 2013, **15**, 7555-7559.
44. C. Y. Chen, M. Wang, J. Y. Li, N. Pootrakulchote, L. Alibabaei, C. H. Ngoc-le, J. D. Decoppet, J. H. Tsai, C. Gratzel, C. G. Wu, S. M. Zakeeruddin and M. Gratzel, *ACS Nano*, 2009, **3**, 3103-3109.
45. K. J. Jiang, N. Masaki, J. B. Xia, S. Noda and S. Yanagida, *Chem Commun (Camb)*, 2006, 2460-2462.
46. L. Schmidt-Mende, J. E. Kroeze, J. R. Durrant, M. K. Nazeeruddin and M. Gratzel, *Nano Lett*, 2005, **5**, 1315-1320.
47. N. L. Fry and P. K. Mascharak, *Acc Chem Res*, 2011, **44**, 289-298.
48. B. Happ, A. Winter, M. D. Hager and U. S. Schubert, *Chem Soc Rev*, 2012, **41**, 2222-2255.
49. P. K. N. Santhanamoorthi, L. Adler-Abramovich, E. Gazit, S. Filipek, Sowmya Viswanathan, Anthony Strzelczyk, V. Renugopalakrishnan, *Adv. Mat. Lett.*, 2011, **2**, 100-105.
50. J. Ryu, S. Y. Lim and C. B. Park, *Adv. Mater.*, 2009, **21**, 1577-1581.
51. X.-y. Wang, A. Del Guerzo and R. H. Schmehl, *J Photoch Photobio C*, 2004, **5**, 55-77.
52. F. Hollmann, I. W. C. E. Arends and K. Buehler, *Chemcatchem*, 2010, **2**, 762-782.

